Available online at www.sciencedirect.com
ScienceDirect
Molecular Phylogenetics and Evolution 41 (2006) 622–635
MOLECULAR PHYLOGENETICS AND EVOLUTION
www.elsevier.com/locate/ympev

Adaptive evolution in mammalian proteins involved in cochlear outer hair cell electromotility

Lucía F. Franchini [a,*], A. Belén Elgoyhen [a,b]

[a] *Instituto de Investigaciones en Ingeniería Genética y Biología Molecular, Consejo Nacional de Investigaciones Científicas y Técnicas, Buenos Aires, Argentina*
[b] *Universidad de Buenos Aires, Buenos Aires, Argentina*

Received 18 February 2006; revised 5 May 2006; accepted 19 May 2006
Available online 6 June 2006

Abstract

Somatic electromotility in cochlear outer hair cells, as the basis for cochlear amplification, is a mammalian novelty and it is largely dependent upon rapid cell length changes proposed to be mediated by the motor-protein prestin, a member of the solute carrier anion-transport family 26. Thus, one might predict that prestin has specifically evolved in mammals to support this unique mammalian adaptation. Using codon-based likelihood models we found evidences for positive selection in the motor-protein prestin only in the mammalian lineage, supporting the hypothesis that lineage-specific adaptation-driven molecular changes endowed prestin with the ability to mediate somatic electromotility. Moreover, signatures of positive selection were found on the α10, but not the α9, nicotinic cholinergic receptor subunits. An α9α10-containing nicotinic cholinergic receptor mediates inhibitory olivocochlear efferent effects on hair cells across vertebrates. Our results suggest that evolution-driven modifications of the α10 subunit probably allowed the α9α10 heteromeric receptor to serve a differential function in the mammalian cochlea. Thus, we describe for the first time at the molecular level signatures of adaptive evolution in two outer hair cell proteins only in the lineage leading to mammals. This finding is most likely related with the roles these proteins play in somatic electromotility and/or its fine tuning.

Keywords: Nicotinic receptors; Acetylcholine; Prestin; Outer hair cells; Hearing; Adaptive evolution

1. Introduction

During the course of Vertebrate evolution two alternative active mechanisms to amplify and tune the auditory response to sound stimuli developed in the hearing organ of the inner ear: an older one relying on the adaptation of the steoreocilia bundle, that has probably persisted in all lineages and a newer one based on voltage-driven somatic electromotility, that appeared only in the mammalian lineage. Since the separation of the three major groups of amniote vertebrates (e.g., mammals, birds–crocodiles, and lizards–snakes) from the stem reptiles approximately 320 million years ago (Kumar and Hedges, 1998), the evolution of the inner ear in those lineages continued independently over long periods of time. Comparative studies suggest that the hearing organ of the earliest vertebrate was small and simple, but possessed hair cell active mechanisms to increase sensitivity, electrical frequency tuning, and incipient micromechanical tuning (Manley, 2000). Though standard stereocilia-based mechanisms to promote amplification may persist in mammals (Chan and Hudspeth, 2005; Jia and He, 2005; Kennedy et al., 2005), an additional mechanism evolved to enhance high frequency sensation. A special cell type, the outer hair cell (OHC) that possesses a remarkably fast somatic mechanical response endows the mammalian cochlea with a unique hearing device which has the capability of detecting a wide range of frequencies including the highest (more than 100 kHz) in the animal world (Manley et al., 2004). Somatic electromotility in OHCs, as the basis for cochlear amplification, is a mammalian novelty and it is largely dependent upon rapid cell length changes in response to receptor potential variations (Ashmore, 1987; Brownell et al., 1985). These length changes are proposed to

* Corresponding author. Fax: +54 11 47868578.
E-mail address: franchini@dna.uba.ar (L.F. Franchini).

1055-7903/$ - see front matter © 2006 Elsevier Inc. All rights reserved.
doi:10.1016/j.ympev.2006.05.042

be mediated by the motor-protein prestin (Zheng et al., 2000), the fifth member of the solute carrier anion-transport family 26 (*SLC26*) (Mount and Romero, 2004). Mutations in this protein lead to non-syndromic hearing loss (Liu et al., 2003). In addition, targeted deletion of the gene encoding prestin, *PRES*, reduces cochlear sensitivity and eliminates both frequency selectivity and OHC somatic electromotility (Everett et al., 2001; Liberman et al., 2002).

Intriguing questions are how this system evolved in the lineage leading to mammals and how the appearance of somatic electromotility is related with the evolution of proteins underlying the functioning of the system. We reasoned that if prestin-driven electromotility was a key step for the evolution of sound amplification and tuning in the mammalian ear, prestin should either be a mammalian novelty or the mammalian protein should have acquired functional features to serve as the OHC motor. We therefore performed a phylogenetic and evolutionary analysis of the *SLC26* super-family in order to establish the context in which prestin evolved and to search for signs of adaptive evolution in *PRES* in the mammalian lineage. Using codon-based likelihood models (Yang, 1998; Yang et al., 2000) we indeed found evidences for positive selection in the motor-protein prestin only in the mammalian lineage, supporting the hypothesis that prestin specifically evolved to support electromotility, a unique mammalian adaptation.

In addition, it has been reported that acetylcholine (ACh) released by olivocochlear (OC) efferent fibers inhibits somatic electromotility in OHCs and thus controls the mammalian cochlear amplifier and the dynamic range of hearing (Dallos et al., 1997; Guinan, 1996). Several studies have shown that a α9α10-containing nicotinic cholinergic receptor (nAChR) mediates efferent effects on hair cells, one of the few verified examples of postsynaptic function for a non-muscle nAChR (Elgoyhen et al., 1994, 2001; Sgard et al., 2002; Vetter et al., 1999). Since cholinergic efferent feedback to hair cells is a common feature among all vertebrates (Guinan, 1996), we expected that the evolutionary history of the genes coding for the α9 and the α10 subunits would look similar along all vertebrate lineages. We found that, as predicted, the α9 subunit is under strong purifying selection in all vertebrate lineages. In contrast, signatures of positive selection were found for the α10 subunit in the mammalian lineage, suggesting the acquisition of novel functional properties for this nAChR subunit.

Our results indicate that mammals have developed not only a new cochlear amplifier based on prestin-dependent electromotility, but also a nAChR at the OC efferent-OHC synapse with unique properties. This nAChR is probably highly tuned to serve a differential function in mammals, due to an evolutionary modified α10 subunit. Thus, we describe for the first time at the molecular level signatures of adaptive evolution in two OHC proteins only in the lineage leading to mammals. This finding is most likely related with the roles these proteins play in OHC somatic electromotility and/or its fine tuning.

2. Materials and methods

2.1. Sequence acquisition

SLC26 sequences were downloaded from the Ensembl database (http://www.ensembl.org). An initial set of *CHRNA* subunits were obtained from The Ligand Gated Ion Channel Database (http://www.ebi.ac.uk/compneur-srv/LGICdb/LGICdb. php Le Novere and Changeux, 1999). The remaining sequences were located via Blast searches (Altschul et al., 1997) in the Ensembl database website using *CHRNA* sequences from other species as queries. Based on sequence similarities and synteny data we assigned each potential *SLC26* family member and *CHRNA* sequences as the ortholog of previously characterized genes.

2.2. Alignment of the sequences

Alignments were performed using the CLUSTALW software (Thompson et al., 1994) implemented in the Vector NTI 8 program (www.invitrogen.com). Similarity was determined by the BLOSUM 62 matrix. Sequence alignments were manually curated and edited using the GeneDoc program (www.cris.com).

2.3. Phylogenetic analyses

Inferences on gene evolution were obtained with the PHYLIP 3.62 Program Package (Felsenstein, 1989). The trees were built using the Neighbor-Joining method (program NEIGHBOR). The distance matrix was built using the PROTDIST program and the model of amino acid substitutions was based on the Jones, Taylor and Thornton model of amino acid change (Jones et al., 1992). The statistical test used to determine the strength of the trees was bootstrap resampling with the SEQBOOT software (1000 replicates; seed: 64238) and the consense tree was calculated by CONSENSE program. The majority-rule consensus trees were constructed by the program DRAWGRAM. The results of CONSENSE analysis after the bootstrap resamplings are written on the node considered.

Trees were edited using TreeView 1.6.6 (http://taxonomy.zoology.gla.ac.uk/rod/treeview.html). For the nAChR phylogenetic reconstruction, the human 5-HT3 subunit was used as the outgroup sequence. For the *SLC26* tree we searched for the closest protein among several anion-transporter families. We selected the *SLC5* family members as the more suitable outgroup for phylogenetic reconstruction. Thus, we included *SLC5A9* protein sequence from mouse (*Mus musculus*) to root the *SLC26* super-family tree.

2.4. Ka/Ks analyses

Ka/Ks ratios were calculated using the DNAsp 4.0 program http://www.ub.es/dnasp and MEGA3. These programs estimate Ka and Ks (the number of synonymous substitutions per synonymous site) for any pair of coding

sequences according to the method of Nei and Gojobori (1986) and Li (1993). Sliding window analyses were performed using DNAsp 4.0 software. We analyzed windows of 90 nucleotides (30 codons) in sliding steps of 9 nucleotides (3 codons). Reconstruction of ancestral sequences was done trough Maximum Likelihood using PAML (Yang, 1997). To build combined Ka/Ks ratio along different lineages, Ka/Ks ratios were added to calculate the combined value.

2.5. Codon-based analysis

In order to detect sites and branches under positive selection, we analyzed the data through the codon-based models developed by Yang and co-workers. (Yang, 1998; Yang and Nielsen, 2002; Yang et al., 2000; Yang and Swanson, 2002) using the program CODEML implemented in PAML (Yang, 1997). These models allow for the selection intensity to vary among amino acid sites and among phylogenetic branches.

Site-specific likelihood models (Nielsen and Yang, 1998; Yang et al., 2000; Yang and Swanson, 2002) which assume variable selective pressures among sites but no variation among branches in the phylogeny were compared as follows: M1 to M2, M7 to M8. M1 (neutral) allows two classes of codons, one with ω over the interval and the other with $\omega = 1$. M2 (selection) is similar to M1 except that it allows an additional class of codons with a freely estimated ω value. M7 estimates ω with a beta-distribution over the interval $(0,1)$, while M8 adds parameters to M7 for an additional class of codons with a freely estimated ω value. Branch-specific likelihood models (Yang, 1998; Yang and Swanson, 2002) consider that all sites in the alignment have the same Ka/Ks ratio, but that there are two different evolutionary scenarios relative to branches: one-ratio model (M0) considers that all branches have the same ω ratio while the two-ratio model establishes that there is a branch (which is predefined) that has a different ratio compared to all other branches. Finally, we applied a branch-site model (Yang and Nielsen, 2002; Yang et al., 2000) to identify positive selected sites in the lineage leading to mammals. Model A considers two kinds of branches (background and foreground) and three kinds of sites. Whereas $\omega 1$ and $\omega 2$ are the only site classes in the background branches, $\omega 3$ considers sites under positive selection in the foreground branch. This model is compared to the neutral model (M1) which assumes two site classes with $0 < \omega 1 < 1$ and $\omega 2 = 1$ in all lineages.

2.6. Rate shift analyses

Functional divergence is defined as changes in protein function between two genes that result in changes in selective constraint at some residues resulting in modified evolutionary rates. Several models have been proposed to test functional divergence among members of protein families (Knudsen and Miyamoto, 2001; Scott et al., 1999). The rationale of these methods is that if statistical analysis shows a significant rate difference between two gene clusters generated by gene duplication, it is possible to predict important amino acid sites displaying rate shifts that could account for the acquisition of a new function. We implemented the method developed by Gu and co-workers (Gu, 2001; Wang and Gu, 2001) using DIVERGE (Gu and Vander Velden, 2002) and the one developed by Knudsen and Miyamoto (2001) implemented trough the publicly available software (www.daimi.au.dk~compbio/rateshift).

3. Results and discussion

3.1. Molecular evolution of the SLC26 family

The phylogenetic tree of Fig. 1 describes the relationships among the urochordate, invertebrate and the eleven vertebrate *SLC26* super-family members including *PRES* (an alignment of the *PRES* sequences used is provided in Supplementary material, Fig. S1). Our analysis supports the inclusion of the fruit fly *Drosophila melanogaster* sequences identified by Weber et al. (2003) and Lohi et al. (2002) as *SLC26* family members. In addition, we included in the analysis, mosquito *Anopheles gambiae* (ag) sequences that we retrieved through Blast searches. Invertebrate sequences form two different groups: *INV1*, more closely related to *SLC26A11*, the most primitive vertebrate member of the family, and *INV2* which seems to be an early branch of the lineage leading to all other vertebrate members of the family. The putative *PRES* ortholog *CG5485* previously identified in *D. melanogaster* (Weber et al., 2003) is a member of *INV2*. However, the analysis we performed indicates that this gene is not more closely related to *PRES* than to other *SLC26* family members. In fact, its location in the tree indicates that this gene could be considered as an invertebrate ancestor of *SLC26A1–SLC26A10* vertebrate genes. Three *CG5485* closely related sequences were found in mosquito, which suggests either that this gene ancestor was duplicated in the lineage leading to mosquito or that some genes were lost in the fruit fly. Additional data analysis is required to address this issue.

Aiming to analyze the early evolution of the family in vertebrates we included in this analysis *SLC26*-related genes we identified in the ascidian *Ciona intestinalis* (Altschul et al., 1997). Ascidians which are members of the clade Urochordate, are along with Vertebrates and the Cephalochordate *Amphioxus*, members of the phylum Chordate. *C. intestinalis* diverged from the last common ancestor of all Chordates about 520 million years ago (Chen et al., 2003). Despite this long evolutionary distance, they exhibit the basic features of the chordate body plan. This has lead to consider Ascidians as key model organisms for understanding the evolution of Vertebrate genomes. The data show that the *C. intestinalis SLC26* family is composed only by a few members (see Fig. 1, ci sequences). The ascidian retrieved sequences appear in the tree as putative ancestors of only three different groups of vertebrate sequences.

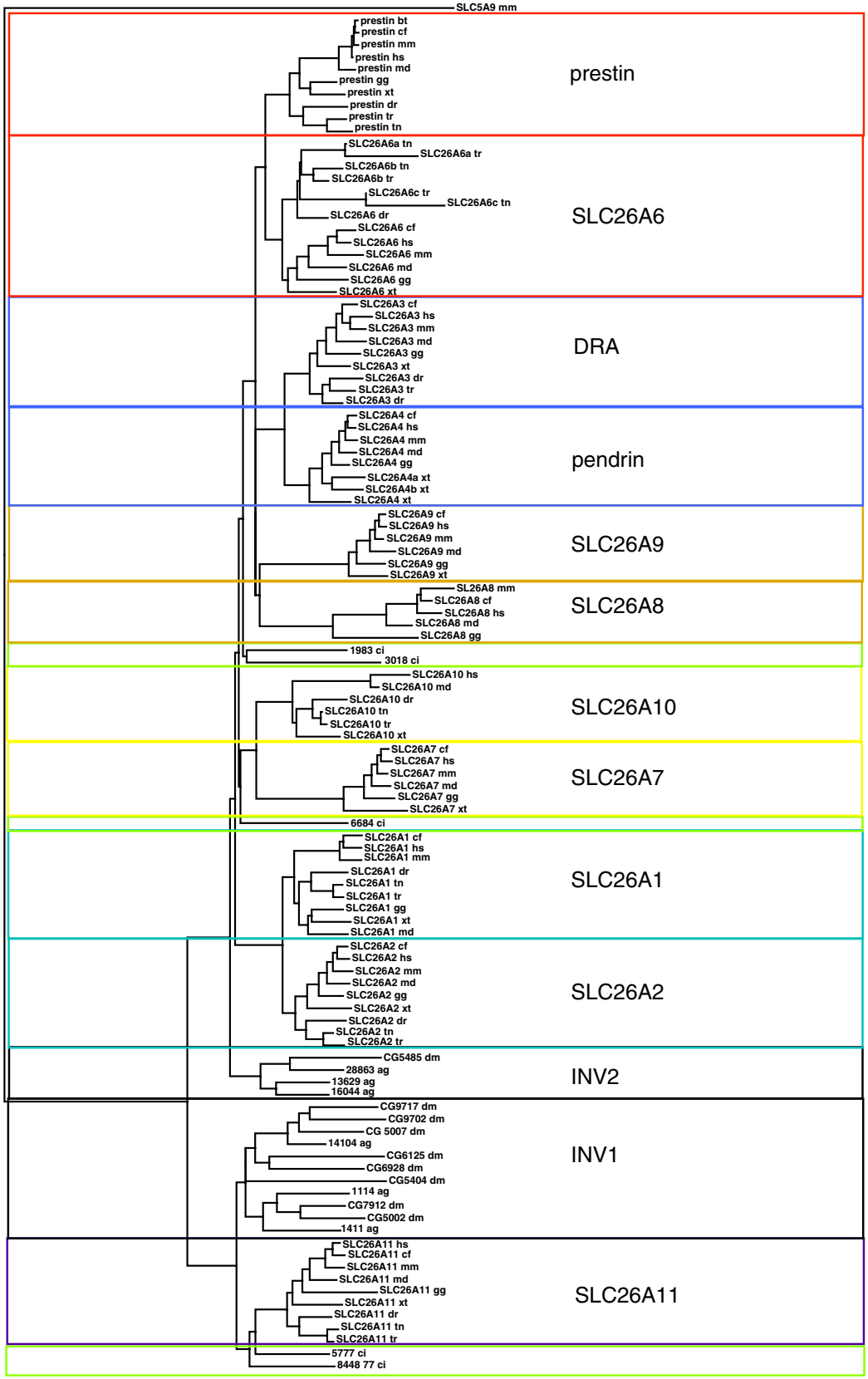

Fig. 1. Phylogenetic analyses of the *SLC26* super-family in Chordates and Invertebrates. Publicly available amino acid sequences were aligned using ClustalW and a Neighbor-Joining tree was generated. Bootstrap values were omitted for clarity. Abbreviations: hs, *Homo sapiens*; mm, *Mus musculus*; cf, *Canis familiaris*; bt, *Bos taurus*; gg, *Gallus gallus*; xt, *Xenopus tropicalis*; tn, *Tetraodon nigroviridis*; tr, *Takifugu rubripes*; dr, *Danio rerio*; dm, *Drosophila melanogaster*; ag, *Anopheles gambiae*; ci, *Ciona intestinalis*.

These data suggest that an expansion of the family occurred in the lineage leading to Vertebrates. This finding is in agreement with the idea that two whole genome duplications occurred early on in vertebrate evolution (Dehal and Boore, 2005).

PRES (*SLC26A5*) most closely related member of the family is *SLC26A6*, a chloride/bicarbonate exchange transporter (Chernova et al., 2005). This gene seems to have been duplicated in pufferfishes, since three putative orthologs were found in fugu (*Takifugu rubripes*; tr) and tetraodon (*Tetraodon nigroviridis*; tn). Since just one copy of this gene was found in zebrafish (*Danio rerio*; dr), it suggests that the duplication occurred after the split of this two fish lineages.

Pendrin (*SLC26A4*) is the fourth member of the family. It is a chloride/iodide transporter and similar to prestin has also been involved in proper ear function (Everett et al., 2001). Pendred's syndrome, a human disease that produces severe hearing impairment, results from mutations in the pendrin encoding gene, *PDS* (Everett and Green, 1999; Everett et al., 2001; Scott et al., 2000; Soleimani et al., 2001). Three paralogs of this gene were found in *Xenopus tropicalis* (xt) in different chromosomal locations (scaffold 452 and scaffold 319). *SLC26A3* also called down regulated in adenoma (*DRA*) is the *PDS* closest related member of the family. *DRA* is a chloride transporter that has been associated with congenital chloride-losing diarrhea (Hoglund et al., 1996). We found two copies of this gene in Chromosome 4 of *D. rerio*, indicating that this gene has been duplicated in this species. *PDS* orthologs were not found in fish suggesting that this gene had a later appearance probably due to *DRA* duplications in the lineage leading to tetrapods after the tetrapod-fish split. This seems to be also the case for *SLC26A7*, *SLC26A8*, *SLC26A9*, since fish orthologs were not found. These three genes have been recently characterized as anion exchangers mediating chloride, sulfate and oxalate transport (Lohi et al., 2002). Whereas *SLC26A7* seems to have derived in the tetrapod lineage from *SLC26A10*, a member of the family poorly characterized, *SLC26A8* and *SLC26A9* appeared after a duplication event from a common ancestor. *SLC26A11* is the vertebrate most primitive member of the super-family and it has been recently shown to be a sodium-independent sulfate transporter (Vincourt et al., 2003). *SLC26A1* or *Sulfate Anion Transporter* 1 (*SAT-1*) and *SLC26A2 Diastrophic Dysplasia Sulfate Transporter* (*DTDST*) seem to be primitive forms from which other members of the super-family have derived. Both are very well characterized sulfate/chloride antiporters (Forlino et al., 2005) and the sulfate transporter signature is very well conserved all across the different species.

The analysis shows that *PRES* orthologs are present in all vertebrate species analyzed, indicating that prestin is not a mammalian exclusive protein. However, in comparison to other families it is noteworthy the high degree of conservation of placental mammal (*Homo sapiens*, *Mus musculus*, *Canis familiaris*) prestin genes. According to the phylogenetic tree they share the highest similarity among all *SLC26* super-family members (Fig. 1). We calculated the percentage of protein identity (% ID) among all vertebrate prestin orthologs used in our study. The data (selected comparisons shown in Table 1) indicate that while placental mammalian sequences share a very high % ID among them, there is a significant drop in identity values when placental mammal sequences are compared to those of non-mammalian vertebrates. In addition, the results indicate that mammalian prestin % ID values are the highest among all members of the super-family (data not shown). In order to compare the evolutionary history of prestin with that of another closely related member of the *SLC26* super-family we selected pendrin, since it has also been involved in proper inner ear function. The results show that % ID values among placental mammal pendrin sequences are not as high as those obtained for prestin (Table 1), suggesting that mammalian prestin has higher selective constraint acting on it. Moreover, identity values between mammals/chicken and mammals/frog comparisons are much higher for pendrin than for prestin, indicating that more molecular changes accumulated in *PRES* than in *PDS* during the same period of time in the mammalian lineage.

Taken together, these results indicate that the vertebrate *SLC26* family has greatly expanded through several

Table 1
Percentage of amino acid identity (% ID) and non-synonymous rate vs. synonymous rate ratio (Ka/Ks) among vertebrate *PRES* and *PDS* genes

		% ID	Ka/Ks	Test of neutrality
PRES				
hs	mm	95.3	0.044	$p < 0.01$
hs	cf	96.4	0.047	$p < 0.01$
hs	md	81.4	0.119	$p < 0.01$
hs	gg	59.1	0.230	$p < 0.01$
hs	xt	57.7	0.133	$p < 0.01$
hs	dr	54.0	0.242	$p < 0.01$
md	gg	61.0	0.218	$p < 0.01$
md	xt	56.6	0.182	$p < 0.01$
md	dr	54.1	0.173	$p < 0.01$
gg	xt	70.9	0.136	$p < 0.01$
gg	dr	58.9	0.131	$p < 0.01$
xt	dr	58.4	0.151	$p < 0.01$
PDS				
hs	mm	87.3	0.115	$p < 0.01$
Hs	cf	90.4	0.118	$p < 0.01$
Hs	md	82.1	0.107	$p < 0.01$
Hs	gg	77.4	0.110	$p < 0.01$
Hs	xt I	65.0	0.181	$p < 0.01$
Hs	xt II	63.3	0.152	$p < 0.01$
md	gg	79.6	0.100	$p < 0.01$
md	xt I	68.2	0.135	$p < 0.01$
md	xt II	64.4	0.156	$p < 0.01$
Gg	xt I	70.1	0.145	$p < 0.01$
Gg	xt II	66.5	0.220	$p < 0.01$
Xt I	xt II	69.6	0.149	$p < 0.01$

p values represent the significance of neutrality test; null hypothesis: Ka = Ks and alternative hypothesis: Ks > Ka. Abbreviations: Ks, synonymous rate; Ka, non-synonymous rate; Ka/Ks, ratio of non-synonymous rate vs. synonymous rate; *PRES*, gene encoding prestin; *PDS*, gene encoding pendrin; hs, *Homo sapiens*; mm, *Mus musculus*; cf, *Canis familiaris*; md, *Monodelphis domestica*; gg, *Gallus gallus*; xt, *Xenopus tropicalis*; dr, *Danio rerio*. xt_ENSXETG00000012196 = xt I; xt_ENSXETG000000220 19 = xt II.

duplication events. The first rounds of duplication probably happened early on in the evolution of this group. Later on, lineage-specific duplication events created new members of the super-family. The expansion of the *SLC26* family has endowed vertebrates with a wide range of specialized anion transporters. In addition, the evolution of prestin in the mammalian lineage has rendered a very specialized protein which is a new type of molecular motor: it has the capability to convert voltage to force using cytoplasmic voltage sensors operating at microsecond rates (Dallos and Fakler, 2002). The appearance of prestin was a key step for the evolution of sound amplification and tuning in the mammalian ear (Manley et al., 2004), therefore *PRES* should show signatures of adaptive evolution in the lineage leading to mammals.

3.2. Signatures of adaptive evolution in mammalian PRES

In order to search for signatures of adaptive evolution in *PRES*, we calculated the ratio of synonymous rate (Ka) vs. non-synonymous rate (Ks), Ka/Ks = ω, among vertebrate orthologs. This ratio measures the pace of protein evolution scaled to mutation rate. Ka/Ks ratios of <1, =1 and >1 indicate purifying selection, neutral evolution and positive or adaptive evolution, respectively. While theoretically adaptive evolution occurs when Ka > Ks, it has been frequently observed when this ratio is around 1 (Crandall et al., 1999; Liberles, 2001). Pairwise Ka/Ks and neutrality test calculations among prestin orthologs indicated that purifying selection is acting on all family members (Table 1). However, as most amino acid sites are expected to be highly conserved among any given family of related proteins and positive selection probably affects just a few sites at very specific time points, using Ka/Ks ratio of the entire protein as an approach to identify positive selection has little power (Yang and Swanson, 2002). Even if a protein is overall under purifying selection, regions of the molecule undergoing positive selection may be identified. In fact, in almost all proteins where positive selection has been demonstrated to be operating, only a few sites were found to be responsible for the adaptive evolution (Hughes and Nei, 1988; Nielsen and Yang, 1998). Aiming to detect prestin domains that underwent adaptive changes in the lineage leading to mammals we conducted a Ka/Ks sliding window analysis (Fig. 2A). Using vertebrate publicly available sequences we deduced the ancestral sequences through the maximum likelihood approach using PAML (Yang, 1997) and obtained a Ka/Ks sliding window profile along *PRES* coding sequences. This analysis showed signatures of adaptive evolution in several regions of the protein in the lineage conducting to mammals. The regions that showed the highest Ka/Ks ratios and the highest number of non-synonymous substitutions were located in the C-teminus of the protein: specifically the Sulfate Transporters and Antisigma Factor Antagonists (STAS) domain which includes the positive and negative charged clusters (Fig. S1).

In order to clearly identify the sites and branches under positive selection in the prestin family among vertebrates we conducted the codon-based neutrality test. The results (Table 2) indicate that the neutral model M1 and the selection model M2 were not significantly different because the extra site class added for the selection model is also evolving at a neutral rate ($\omega 3 = 1$). No sites under positive selection were detected. The discrete model (M3) with 3 site classes ($k = 3$) fits the data significantly better than the one-ratio model M0 ($\mathrm{LRT} = 2 \times 214.16 = 428.32$; $\mathrm{df} = 2$; $p < 0.005$) but does not suggest any class of sites under positive selection. Model 8 does not fit the data significantly better than M7 ($\mathrm{LRT} = 2 \times 0.43 = 0.86$; $\mathrm{df} = 2$; $p < 0.75$).

We next applied a branch-specific likelihood analysis to prestin data (Yang, 1998). When model M0 (which considers that all branches have the same ω ratio) and the two-ratio model (which establishes that the branch conducting to mammals has a different ratio) were compared trough a LRT, the results indicated that the two-ratio model fits the data significantly better ($\mathrm{LRT} = 2 \times 14.88 = 29.76$; $\mathrm{df} = 1$; $p < 0.001$) suggesting that the lineage leading to mammals evolved at a faster rate ($\omega 2 = 1.2$) compared to other lineages in the family ($\omega 1 = 0.09$).

In addition, our analysis indicates that the branch-site model A (Yang and Nielsen, 2002) fits the data significantly better than the neutral model M0 and identified 19 sites ($P > 0.95$) and 31 sites ($0.90 < P < 0.95$) to be under positive selection in the lineage conducting to mammals (Fig. 2A and Fig. S1). For the sake of comparison, we analyzed the data considering the foreground lineage the branch conducting to *G. gallus*. Even though, a two-branch model fits the data significantly better than the one ratio model M0 ($\mathrm{LRT} = 2 \times 7.28 = 14.56$; $\mathrm{df} = 2$; $p < 0.005$), model A does not fit the data significantly better than the neutral model M1 ($\mathrm{LRT} = 2 \times 1.77 = 3.54$; $\mathrm{df} = 2$; $p = 0.25$) and does not detect any sites under positive selection. Taken together the analysis suggests that only the lineage leading to mammalian prestin has undergone adaptive evolution.

Sites identified by model A are located in some key areas of the prestin protein like the Na/diCo symport region, the sulfate transport signature, the transmembrane regions (TM1, TM4, TM5) and in the STAS domain (see Fig. 2A and Fig. S1). Some changes that lead to non-conservative amino acid substitutions and have the potential to produce dramatic changes in the chemical properties of the protein are noteworthy: C124T (C/T mammalian/other vertebrate lineages; positions correspond to the human sequence) in the sulfate transporter signature or M225Q in TM4 and C260V in TM5 (see Fig. S1). Previous reports have shown that even though nearly the full length protein is required for normal prestin expression and function, some amino acids in the C-terminus play a key role in prestin cellular distribution (Zheng et al., 2005). Our sequence analysis showed that while the whole C-terminal region is highly conserved among placental mammals, some major changes are observed when compared to chicken, frog and fish orthologs (see alignment Fig. S1). In addition, within the

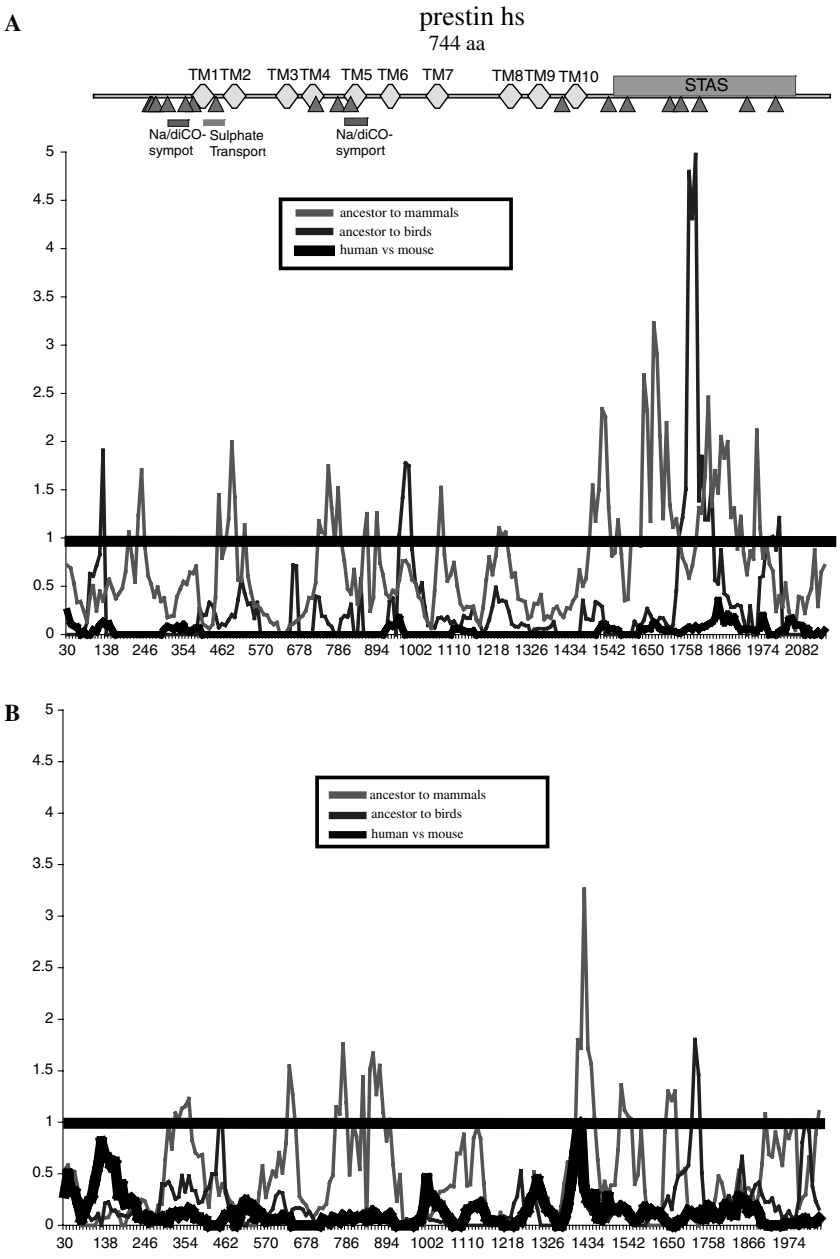

Fig. 2. Sliding window analysis of Ka/Ks along *PRES* (A) and *PDS* (B) coding regions. Peaks above the black line have Ka/Ks greater than 1 and therefore indicate an excess of non-synonymous substitutions over neutral expectations. The lineage leading to mammals is defined as the lineage from the last common ancestor after the bird/mammal split to mammals. A schematic representation of prestin shown above (A) indicates the location of positively selected sites (green arrows) along the transmembrane and functional domains of the protein. (For interpretation of the references to colours in this figure legend, the reader is referred to the web version of this paper.)

STAS domain seven strong positively selected sites ($P > 0.95$) were detected. Moreover, a striking difference between mammals and non-mammalian sequences is the absence in the latter of the negative charged cluster (Fig. S1). Codon-based analysis detected a strong positively selected site (E613N/I) within this region. On the other hand, mammals lack a lysine and arginine rich region that could account for a second positively charged cluster. A recent work has shown that the region between amino acids 725 and 745 (positions corresponding to human sequence, Fig. S1) is key for the proper membrane targeting of prestin (Zheng et al., 2005), a property which is essential for a protein that has to be highly packed in the lateral plasma membrane to serve its motor function. Our sequence analysis indicates that even though this region is highly conserved among mammals, non-mammalian proteins totally lack conservation when compared to mammalian sequences or among them (Fig. S1). Although evolutionary conserved regions are functionally important, molecular innovations that provide adaptive changes are the mechanisms

Table 2
Likelihood values and parameter estimates under models of variable ω ratios among sites for *PRES* and *CHRNA9/10*

Model code	*PRES*				*CHRNA9/10*			
	Log Likelihood	Estimates of parameters			Log Likelihood	Estimates of parameters		
M0 (one-ratio)	−10951.40	$\omega = 0.11$			−14146.01	$\omega = 0.05$		
Branch-specific models								
Two-ratios	−10934.22	$\omega1 = 0.09$	$\omega2 = 1.20$		−14135.70	$\omega1 = 0.09$	$\omega2 = 0.02$	
Site-specific models								
M1 (neutral)	−10830.24	$p1 = 0.82$	$p2 = 0.18$		−13572.71	$p1 = 0.65$	$p2 = 0.34$	
		$\omega1 = 0.08$	$\omega2 = 1.00$			$\omega1 = 0.05$	$\omega2 = 1.00$	
M2 (selection)	−10830.24	$p1 = 0.82$	$p2 = 0.17$	p3 = 0.01	−13572.71	$p1 = 0.65$	$p2 = 0.12$	$p3 = 0.22$
		$\omega1 = 0.08$	$\omega2 = 1.00$	$\omega3 = 1.00$		$\omega1 = 0.05$	$\omega2 = 1.00$	$\omega3 = 1.00$
M3 (discrete)	−10737.23	$p1 = 0.48$	$p2 = 0.37$	$p3 = 0.14$	−13422.58	$p1 = 0.38$	$p2 = 0.33$	$p3 = 0.28$
		$\omega1 = 0.01$	$\omega2 = 0.15$	$\omega3 = 0.44$		$\omega1 = 0.004$	$\omega2 = 0.10$	$\omega3 = 0.62$
M7 (beta)	−10737.16	$\boldsymbol{p} = 0.47$	$\boldsymbol{q} = 3.21$		−13415.48	$\boldsymbol{p} = 0.26$	$\boldsymbol{q} = 0.98$	
M8 (beta & ω)	−10737.12	$\boldsymbol{p} = 0.48$	$\boldsymbol{q} = 3.32$		−13408.20	$\boldsymbol{p} = 0.32$	$\boldsymbol{q} = 2.08$	
		$p1 = 0.997$	$p2 = 0.003$	$\omega2 = 1.09$		$p1 = 0.88$	p2 = 0.11	$\omega2 = 1.43$
Branch-site models								
Model A	−10796.53	$p1 = 0.53$	$p2 = 0.23$	$p3 = 0.24$	−13537.07	$p1 = 0.55$	$p2 = 0.30$	$p3 = 0.14$
		$\omega1 = 0.06$	$\omega2 = 1.00$	$\omega3 = 1.38$		$\omega1 = 0.05$	$\omega2 = 1.00$	$\omega3 = 53.33$

Abbreviations: ω = Ka/Ks; $p1$–$p3$ = propotion of sites; $\boldsymbol{p}$ and $\boldsymbol{q}$: parameters of the beta distribution.

underlying the invention of new protein functions. Thus, positively selected sites must have provided prestin with new functional capacities endowing mammals with a selective advantage in their auditory function. This is in accordance with the observation that prestin-based somatic electromotility in OHCs, as the basis for cochlear amplification is a mammalian novelty (Ashmore, 1987; Brownell et al., 1985), a mechanism that most likely evolved to enhance high frequency sensation (Manley et al., 2004).

For the sake of comparison, we performed a search for evidences of positive selection using pendrin sequences. Ka/Ks analysis showed that unlike prestin, pendrin mammalian sequences had less selective constraint acting on them (Table 1). This observation is in agreement with the smaller identity values found for the mammalian pendrin sequences compared to the highly conserved prestin mammalian sequences. A Ka/Ks window analysis indicated that even though some peaks showed Ka/Ks values higher than 1 along the pendrin sequences, the region containing the highest peak is highly variable in all the species analyzed, including mammals (see human vs. mouse profile, Fig. 2B). On the other hand, sequence analysis indicated that the STAS region that has dramatically changed in mammalian prestin is strongly conserved among all pendrin sequences analyzed. Thus, contrary to that obtained for prestin, there was no overt evidence of adaptive evolution acting on pendrin.

3.3. Rate shift analysis

Using DIVERGE we calculate the coefficient of functional divergence (θ) between mammalian prestin genes and its more closely related member of the *SLC26* family (*SLC26A6*). This analysis provides significant support to the functional divergence hypothesis ($\theta = 0.527 \pm 0.082$; LRT Theta = 41.541494). In addition, we identified 20 sites [$P(S1|X) > 0.60$] showing rate shift between these two proteins (see Fig. S1). We tested for functional divergence between mammal and non-mammal prestin genes and we found no evidence to support functional divergence ($\theta = 0.080 \pm 0.073$; LRT Theta = 1.190). However, since the majority of sites are highly conserved among prestin genes, especially in the transmembrane domain, this method can lack power to detect functional divergence (Gu and Vander Velden, 2002). On the other hand, the maximum likelihood method developed by Knudsen and Miyamoto (2001) applied to prestin data (mammals vs. non-mammals) identified 23 sites with significant rate shift and 46 slow rate sites at the 5% level (see Fig. S1). Rate shift sites are located in functional sites of prestin such us the Na/diCO-symport, sulfate transport, transmembrane regions (TM1, TM2, TM5, TM6 and TM7) and the STAS domain. These data indicate that mammalian prestin functionally diverged from its closest related *SLC26* family member (*SLC26A6*) and also that many residues in mammalian prestin functionally diverged from non-mammalian prestin. All together these findings provide further support to our hypothesis suggesting that prestin acquired a mammalian-specific function.

3.4. Molecular evolution of the α9 and α10 nAChR subunits in vertebrates

The α9 and α10 nAChR subunits assemble to form the receptor that mediates synaptic transmission between efferent OC fibers and hair cells of the cochlea (Elgoyhen et al., 1994, 2001; Sgard et al., 2002). They are the latest vertebrate nAChR subunits that have been cloned and their identification has established a distant early divergent branch within the nAChR gene family (Le Novere et al., 2002). The α10

subunit serves as a 'structural' component leading to heteromeric α9α10 nAChRs with distinct properties. Since efferent cholinergic innervation of hair cells has been described along all vertebrates (Guinan, 1996) we expected that the evolutionary history of the genes coding for the α9 and the α10 subunits would look similar along all vertebrate lineages.

As shown on the phylogenetic tree of Fig. 3 (an alignment of the α10 sequences used is provided in Fig. S2), mammalian α10 subunits constitute a separated clade or subfamily (group IV) within the α9/α10 family. It is noteworthy that previously identified chicken α10 is part of another group (III) containing fish and frog α9c and d sequences. While sequence identities makes it difficult to establish the ortholog genes encoding α10 subunits *(CHRNA10)* among the several *CHRNA9*-like genes in other vertebrates, a synteny analysis has allowed us to define that the genes encoding the proteins conforming group III are *CHRNA10* orthologs (data not shown). These data suggest that mammalian *CHRNA10* had a separated evolutionary history within the family. The analysis of the % ID among all members of the α9/α10 family (Table 3) indicated that both placental mammal α9 and α10 subunits show high % ID values. In contrast the marsupial α9 compared to any non-mammal α9 renders much higher identity values than the equivalent comparison between α10 subunits; e.g., α9 marsupial-chicken 82.7% vs. α10 marsupial-chicken 67.6%. In addition, it is worth mentioning that the identity between α9 and α10 is much higher for chicken (65%) than for mammals (54.2%). Taken together, these results suggest that while α10 subunits underwent a significant amount of changes in the lineage conducting to mammals, α9 has been very well conserved since its appearance. Previous works have assigned all subunits cloned from fish as α9 and not as α10 based on their higher similarity to α9 mammalian subunits (Drescher et al., 2004; Jones et al., 2003). According to our more inclusive and extensive work fish α9cs and α9ds are more similar to the chicken α10 subunit than to the canonical mammalian and chicken α9. They form clade III which includes the chicken α10 subunit.

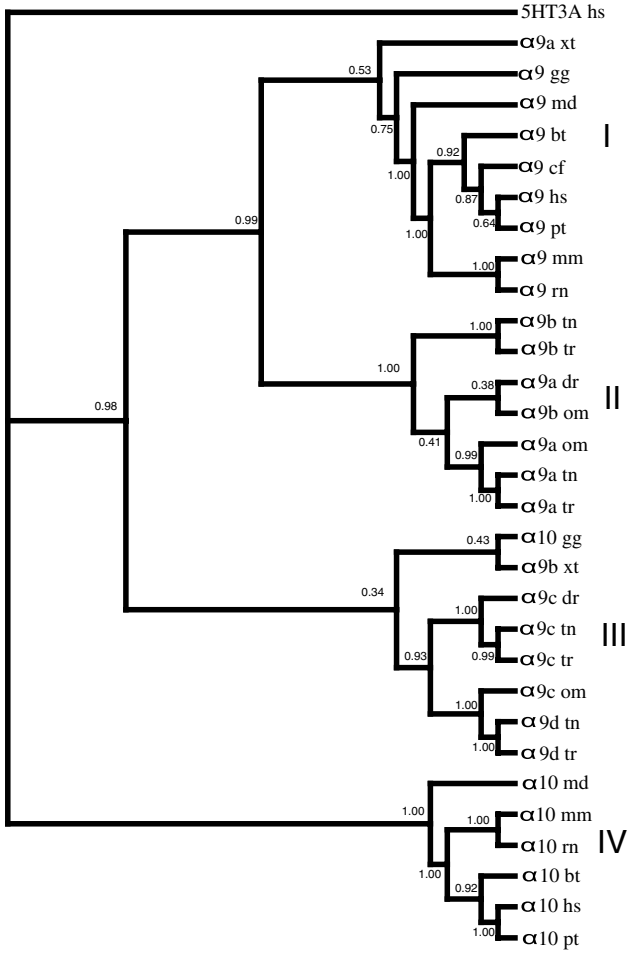

Fig. 3. Phylogenetic analyses of the *CHRNA9* and *CHRNA10* orthologs in vertebrates. Publicly available amino acid sequences were aligned using ClustalW and a Neighbor-Joining tree was generated. Bootstrap values are indicated. Abbreviations: hs, *Homo sapiens*; pt, *Pan troglodytes*; bt, *Bos Taurus*; cf, *Canis familiaris*; mm, *Mus musculus*; rn, *Rattus norvergicus*; md, *Monodelphis domestica*; gg, *Gallus gallus*; xt, *Xenopus tropicalis*; tn, *Tetraodon nigroviridis*; tr, *Takifugu rubripes*; dr, *Danio rerio,* om, *Oncorhyncus mykiss.*

Table 3
Percentage of amino acid identity (% ID) and non-synonymous rate vs. synonymous rate ratio (Ka/Ks) among vertebrate *CHRNA9* and *CHRNA10* genes

		% ID	Ka/Ks	Test of neutrality
CHRNA9				
hs	mm	90.8	0.066	$p < 0.01$
hs	bt	95.9	0.084	$p < 0.01$
hs	cf	95.4	0.081	$p < 0.01$
hs	md	89.1	0.060	$p < 0.01$
hs	gg	73.9	0.046	$p < 0.01$
hs	xt a	69	0.093	$p < 0.01$
hs	tn a	64.5	0.152	$p < 0.01$
md	gg	82.7	0.057	$p < 0.01$
md	xt a	76.1	0.110	$p < 0.01$
md	tn	72.7	0.087	$p < 0.01$
gg	xt a	72.6	0.067	$p < 0.01$
gg	tn a	67.5	0.077	$p < 0.01$
xt a	tn a	68.9	0.147	$p < 0.01$
CHRNA10				
hs	mm	91.6	0.076	$p < 0.01$
hs	bt	93.7	0.097	$p < 0.01$
hs	md	78.5	0.135	$p < 0.01$
hs	gg	66.5	0.354	$p < 0.01$
hs	xt b	58.5	0.206	$p < 0.01$
hs	tn d	58	0.354	$p < 0.01$
md	gg	67.6	0.270	$p < 0.01$
md	xt b	59.2	0.225	$p < 0.01$
md	xt b	58.5	0.232	$p < 0.01$
gg	xt b	73.3	0.067	$p < 0.01$
gg	tn d	69.1	0.320	$p < 0.01$
xt b	tn d	70.5	0.122	$p < 0.01$
CHRNA9 hs	*CHRNA10* hs	54.2	—	—
CHRNA9 md	*CHRNA10* md	57.9	—	—
CHRNA9 gg	*CHRNA10* gg	65.0	—	—

p values represent the significance of neutrality test; null hypothesis: Ka = Ks and alternative hypothesis: Ks > Ka. Abbreviations: Ks, synonymous rate; Ka, non-synonymous rate; Ka/Ks, ratio of non-synonymous rate vs. synonymous rate; *CHRNA*, nicotinic receptor alpha subunit; hs, *Homo sapiens*; mm, *Mus musculus*; md, *Monodelphis domestica*; gg, *Gallus gallus*; xt, *Xenopus tropicalis*; tn, *Tetraodon nigroviridis*.

Moreover, based on synteny analysis we have established that they are in fact the *CHRNA10* orthologs (data not shown). We therefore propose to name these genes of tetraodon and fugu as *CHRNA10*.

The present data suggest a possible scenario for the evolution of these nicotinic receptor subunits: after a duplication event that created the *CHRNA9* and *CHRNA10* ancestors, these two genes co-existed without much functional differentiation. Then at some point, most probably in the lineage leading to mammals, amino acid changes started to accumulate rapidly producing *CHRNA10* to diverge from *CHRNA9*. If this divergence was produced by a relaxation in selective pressure or, on the contrary, it was actually shaped by positive selection, is an open question. To shed light on the evolutionary history of these nicotinic receptor subunits we searched for signatures of positive selection in the *CHRNA9* and *CHRNA10* genes.

3.5. Signatures of adaptive evolution in the mammalian α10 subunit

In order to assess if the increased amount of changes in the α10 subunits suggested by the comparison of identity values was the result of positive selection acting on the *CHRNA10* gene, we calculated the Ka/Ks ratio among all *CHRNA9* and *CHRNA10* genes. Our results (Table 3) show that while any placental mammalian *CHRNA10* sequence comparison produced Ka/Ks values indicating strong purifying selection, any mammalian sequence compared to chicken *CHRNA10* or any sequence included in clade III (see Fig. 3) always produced higher Ka/Ks values. In contrast, the same analyses conducted on *CHRNA9* sequences indicate that this gene is under high selective constraint in all the species analyzed from fish to mammals.

To further analyze the evolution of these genes in the lineage conducting to mammals, we obtained a Ka/Ks sliding window profile along different evolutionary lineages in order to identify fast evolving regions in the *CHRNA10* coding sequence (Fig. 4A). The analysis clearly identified several *CHRNA10* regions with values greater than one in the lineage conducting to mammals and in the bird lineage. A careful examination of the sequences indicated that the regions with higher Ka/Ks in these two lineages are different. Among the functional domains showing high Ka/Ks values only in mammals, two correspond to the ACh-binding site and other two to transmembrane regions I and IV, domains that are relatively highly conserved among members of the nAChR family (Karlin, 2002). Peaks with high Ka/Ks values in the mammalian as well as in the chicken *CHRNA10* were also observed in the regions corresponding to the signal peptide and the cytoplasmic loop, an expected result since these regions are the most variable between nAChR ortholog genes. The non-synonymous changes observed in several *CHRNA10* regions could represent both, relaxed functional constraint or Darwinian positive selection acting in these areas. However, due to the high level of conservation of the regions forming the ACh-binding pocket and the transmembrane domains within the canonical α9 and within mammalian α10 subunits, relaxed functional constraint is unlikely.

The Ka/Ks sliding window analysis on *CHRNA9* (Fig. 2B) indicates that a higher selective constraint is acting on *CHRNA9* genes. In the profile generated for the lineage conducting to mammals, we found a unique peak greater than 1. Again, this fast evolving or relaxed region corresponds to the cytoplasmic loop, the least conserved sequence among all nAChR subunits (Karlin, 2002).

3.6. Codon-based analysis

In order to clearly identify the sites and branches under positive selection in the *CHRNA9*/*CHRNA10* family among vertebrates we conducted the same codon-based neutrality test applied to *PRES* sequences. The results (Table 2) indicated that the neutral model M1 and the selection model M2 are not different. The discrete model M3 with $k = 3$ site classes fits the data significantly better than the one-ratio model M0 but does not suggest any class of sites under positive selection. Model 8 fits the data significantly better than M7 ($\mathrm{LRT} = 2 \times 7.28 = 14.56$; $\mathrm{df} = 2$; $p < 0.05$) and suggests 11% of sites to be under positive selection with $\omega = 1.43$. The Bayesian approach identified 13 sites under positive selection ($0.5 < P < 0.9$), however they are all located in the hypervariable cytoplasmic loop.

Aiming to test the hypothesis that the mammalian lineage evolved at a different rate, we next applied the branch-specific likelihood analysis to the *CHRNA9*/*CHRNA10* data. The results indicate that the two-branch model fits the data significantly better ($\mathrm{LRT} = 2 \times 10.31 = 20.62$; $\mathrm{df} = 1$; $p < 0.005$) than the one establishing all the lineages evolving at the same rate (M0, one rate). This result indicates that the mammalian lineage evolved at a different rate after the mammalian-bird split, however the Ka/Ks ratio ($\omega 2$, Table 2) in this lineage is not indicative of positive selection. Finally, we applied the branch-site model, which considers the branch leading to mammals as the foreground branch while all other branches are considered as background branches. Our data indicate that Model A fits the data significantly better than the neutral model M1 ($2 \times 106.63 = 213.26$; $\mathrm{df} = 2$; $p < 0.005$) and identified 17 sites ($P > 0.9$) to be under strong positive selection in the lineage conducting to mammals. Sites identified by this model are located in some key areas of the α10 subunit: Loop E, Loop B, Cys Loop and TM1. We applied the same analysis to the data considering as foreground lineage the one conducting to chicken *CHRNA10*. The analysis indicates that even though there is an improvement in the fitting of the model to the data when considering this branch as evolving to a different rate, the neutral model M1 fits the data significantly better than model A. Thus, it was possible to find signatures of adaptive evolution at selected sites only in the mammalian *CHRNA10*, suggesting that in this animal group this protein has been shaped by positive Darwinian selection.

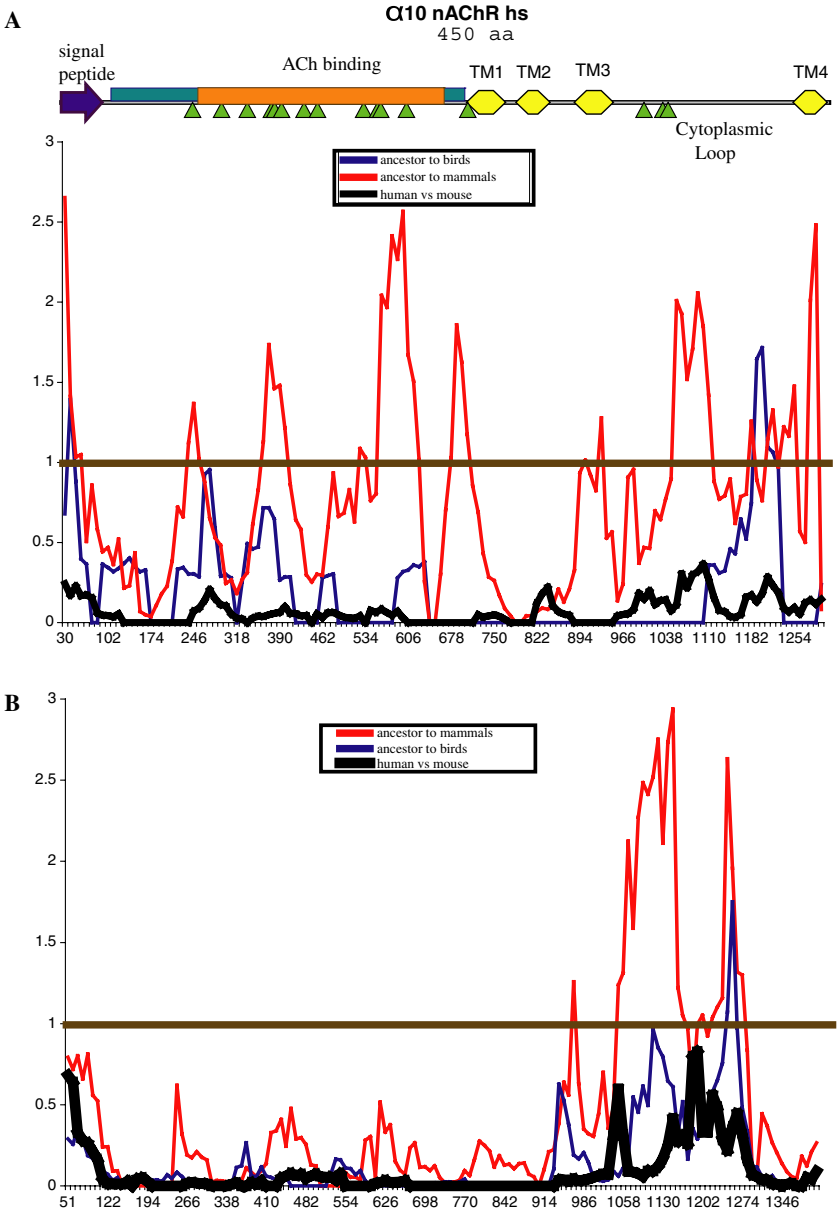

Fig. 4. Sliding window analysis of Ka/Ks along *CHRNA10* (A) and *CHRNA9* (B) coding regions. Peaks above the black line have Ka/Ks greater than 1 and therefore an excess of non-synonymous substitutions over neutral expectations. The lineage leading to mammals is defined as the lineage from the last common ancestor after the bird/mammal split to mammals. A schematic representation of α10 nAChR subunit shown above (A) indicates the location of positively selected sites (green arrows) along the different domains of the protein. (For interpretation of the references to colours in this figure legend, the reader is referred to the web version of this paper.)

Many strong positively selected sites in key functional areas in the *CHRNA10* mammalian lineage were detected through codon-based methods (Fig. 3 and Fig. S2). These results strongly argue that positive selection has driven amino acid changes in *CHRNA10* but not in *CHRNA9*, along the lineage conducting to mammals. One could speculate that the acquired evolutionary changes might have resulted in the acquisition of a new function in the mammalian α10 nAChR subunit. Since both *CHRNA10* and *CHRNA9* are under strong purifying selection in mammals, the functional split between α9 and α10 nAChR mammalian subunits is being maintained because of the critical role these proteins might play in the α9α10 nAChR of OHCs. In this regard, it has been demonstrated that although rat homomeric α9 receptors are functional, the α10 subunit serves as a 'structural' component leading to heteromeric α9α10 nAChRs with desensitization kinetics, current–voltage dependency and sensitivity to extracellular Ca^{2+} that differ from those of homomeric α9 receptors (Elgoyhen et al., 1994, 2001; Katz et al., 2000; Weisstaub et al., 2002). Several positively selected sites were detected in different domains of the mammalian α10 that participate in the conformation of the ACh-binding site. In particular, a R143M/T substitution (mammalian to clade III substitution, numbering according to the human sequence), which renders a positively charged residue in the mammalian α10 subunit at

a site that has been identified to form part of Loop E of the binding site (Brejc et al., 2001; Celie et al., 2004). In addition, substitution S131E/D located in the vicinity of Loop E, locates a neutral amino acid in mammalian α10 compared to a negatively charged residue in the clade III subunits. Negatively charged residues within or near Loop E are the probable source of the negative electrostatic potential in the ACh-binding site of the receptor, and their movement towards a bound quaternary ammonium group could be part of the activation mechanism (Karlin, 2002).

In addition, positively selected sites were observed in regions involved in channel gating. The gating properties of ion channels are crucial to shape their physiologic response. In nAChRs such gating properties are directly related to the subunit composition (Bouzat et al., 1994). It has been reported that the interplay between the β1–β2, Cys-, β8–β9 and TM2–TM3 loops and the beginning of TMI (see Fig. S2) couples the conformational change at the agonist binding site to the ion pore, and conversely, couples the functional state of the pore to the binding site (Bouzat et al., 2004). A conserved small residue, A161, in the mammalian α10 Cys-loop is substituted for residues Y/F in species forming clade III. Moreover, a R203E substitution, changes a positively to a negatively charged residue at loop β8–β9. Finally, an A238F substitution introduces a hydrophobic residue at the beginning of TMI in clade III α10 subunits.

One could raise the hypothesis that the acquired changes in the mammalian α10 subunit result in a α9α10 nAChR with gating kinetics highly tuned to serve a differential function in cochlear OHCs, e.g., modulation of electromotility. If as deduced from our analysis, mammalian α10 shows signatures of adaptive evolution over clade III α10 subunits, the properties of receptors assembled from the latter and their α9 partners should differ from those described for the rat α9α10 nAChR (Elgoyhen et al., 2001; Katz et al., 2000; Weisstaub et al., 2002). Further experimental data will test this hypothesis.

3.7. Rate shift analysis

Using DIVERGE we calculated the coefficient of functional divergence between α9 and α10 gene clusters. The data indicate that mammalian α10 sequences (group IV Fig. 3) show significant evidences for functional divergence when compared to any other group of α9 genes (groups I, II, III, Fig. 3): group IV vs. I: ($\theta = 0.522 \pm 0.099$, LRT = 27.773; group IV vs. II: $\theta = 0.455 \pm 0.113$, LRT = 16.126; group IV vs. III: $\theta = 0.497 \pm 0.097$, LRT = 26.257). Using posterior probability we detected eighty four critical amino acid residues [$P(S1|X) > 0.65$] responsible for type I functional divergence between mammalian α9 and α10 clusters (see Fig. S2).

In addition, using the method developed by Knudsen and Miyamoto (2001) we compared mammalian α10 and group III genes and identified 16 sites with significant rate differences and 23 slow rate sites at the 5% level (see Fig. S2). Several key functional sites show both, strong signatures of positive selection in the lineage leading to mammals and also significant rate shift (see Fig. S2). These data suggest that in these sites functional divergence has been driven by adaptive evolution. These findings are consistent with our hypothesis suggesting that α10 acquired a new function in mammals.

4. Conclusion

We provide evidence for positive selection and functional divergence for two mammalian OHC genes: the motor-protein prestin and the α10 nAChR. Prestin underwent some dramatic changes in its primary sequence after the split between mammals and birds. In addition, our data indicates that in placental mammals this gene is under strong purifying selection, suggesting that its function is highly important for these organisms' fitness and adaptation. This result sheds additional evidence towards the importance of prestin-based voltage-driven somatic electromotility in mammals. On the other hand, the α10 nAChR subunit (but not α9) shows signatures of positive Darwinian selection only along the lineage conducting to mammals, suggesting the possible acquisition of new functions for this receptor subunit rendering a nAChR with unique characteristics in mammalian OHCs. In the light of our data, we hypothesize that the duplication of *CHRNA9* in a fish ancestor created *CHRNA10*. Later on, in the lineage conducting to mammals, this gene underwent accelerated evolution acquiring a new function different from *CHRNA9*. This hypothesis is also strongly supported by our functional divergence analysis. Thus, we describe at the molecular level signatures of adaptive evolution for two OHC proteins in the lineage leading to mammals. This finding is most likely related with the roles these proteins play in OHC somatic electromotility and/or its fine tuning.

Acknowledgment

This work was supported by an International Research Scholar Grant from the Howard Hughes Medical Institute, a Research Grant from ANPCyT (Argentina) and a Research Grant from Universidad de Buenos Aires to ABE. We thank Fundación Antorchas, Argentina and the International Brain Research Organization for the support to LFF. We want to thank Dr. Paul Fuchs for suggestions in the presentation of the data.

Appendix A. Supplementary data

Supplementary data associated with this article can be found, in the online version, at doi:10.1016/j.ympev. 2006.05.042.

References

Altschul, S.F., Madden, T.L., Schaffer, A.A., Zhang, J., Zhang, Z., Miller, W., Lipman, D.J., 1997. Gapped BLAST and PSI-BLAST: a new

generation of protein database search programs. Nucleic Acids Res. 25, 3389–3402.

Ashmore, J.F., 1987. A fast motile response in guinea-pig outer hair cells: the cellular basis of the cochlear amplifier. J. Physiol. 388, 323–347.

Bouzat, C., Bren, N., Sine, S.M., 1994. Structural basis of the different gating kinetics of fetal and adult acetylcholine receptors. Neuron 13, 1395–1402.

Bouzat, C., Gumilar, F., Spitzmaul, G., Wang, H.L., Rayes, D., Hansen, S.B., Taylor, P., Sine, S.M., 2004. Coupling of agonist binding to channel gating in an ACh-binding protein linked to an ion channel. Nature 430, 896–900.

Brejc, K., van Dijk, W.J., Klaassen, R.V., Schuurmans, M., van Der Oost, J., Smit, A.B., Sixma, T.K., 2001. Crystal structure of an ACh-binding protein reveals the ligand-binding domain of nicotinic receptors. Nature 411, 269–276.

Brownell, W.E., Bader, C.R., Bertrand, D., de Ribaupierre, Y., 1985. Evoked mechanical responses of isolated cochlear outer hair cells. Science 227, 194–196.

Celie, P.H., van Rossum-Fikkert, S.E., van Dijk, W.J., Brejc, K., Smit, A.B., Sixma, T.K., 2004. Nicotine and carbamylcholine binding to nicotinic acetylcholine receptors as studied in AChBP crystal structures. Neuron 41, 907–914.

Chan, D.K., Hudspeth, A.J., 2005. Ca^{2+} current-driven nonlinear amplification by the mammalian cochlea in vitro. Nat. Neurosci. 8, 149–155.

Chen, J.Y., Huang, D.Y., Peng, Q.Q., Chi, H.M., Wang, X.Q., Feng, M., 2003. The first tunicate from the Early Cambrian of South China. Proc. Natl. Acad. Sci. USA 100, 8314–8318.

Chernova, M.N., Jiang, L., Friedman, D.J., Darman, R.B., Lohi, H., Kere, J., Vandorpe, D.H., Alper, S.L., 2005. Functional comparison of mouse slc26a6 anion exchanger with human SLC26A6 polypeptide variants: differences in anion selectivity, regulation, and electrogenicity. J. Biol. Chem. 280, 8564–8580.

Crandall, K.A., Kelsey, C.R., Imamichi, H., Lane, H.C., Salzman, N.P., 1999. Parallel evolution of drug resistance in HIV: failure of nonsynonymous/synonymous substitution rate ratio to detect selection. Mol. Biol. Evol. 16, 372–382.

Dallos, P., Fakler, B., 2002. Prestin, a new type of motor protein. Nat. Rev. Mol. Cell Biol. 3, 104–111.

Dallos, P., He, D.Z., Lin, X., Sziklai, I., Mehta, S., Evans, B.N., 1997. Acetylcholine, outer hair cell electromotility, and the cochlear amplifier. J. Neurosci. 17, 2212–2226.

Dehal, P., Boore, J.L., 2005. Two rounds of whole genome duplication in the ancestral vertebrate. PLoS Biol. 3, e314.

Drescher, D.G., Ramakrishnan, N.A., Drescher, M.J., Chun, W., Wang, X., Myers, S.F., Green, G.E., Sadrazodi, K., Karadaghy, A.A., Poopat, N., Karpenko, A.N., Khan, K.M., Hatfield, J.S., 2004. Cloning and characterization of alpha9 subunits of the nicotinic acetylcholine receptor expressed by saccular hair cells of the rainbow trout (*Oncorhynchus mykiss*). Neuroscience 127, 737–752.

Elgoyhen, A.B., Johnson, D.S., Boulter, J., Vetter, D.E., Heinemann, S., 1994. Alpha 9: an acetylcholine receptor with novel pharmacological properties expressed in rat cochlear hair cells. Cell 79, 705–715.

Elgoyhen, A.B., Vetter, D.E., Katz, E., Rothlin, C.V., Heinemann, S.F., Boulter, J., 2001. alpha10: a determinant of nicotinic cholinergic receptor function in mammalian vestibular and cochlear mechanosensory hair cells. Proc. Natl. Acad. Sci. USA 98, 3501–3506.

Everett, L.A., Belyantseva, I.A., Noben-Trauth, K., Cantos, R., Chen, A., Thakkar, S.I., Hoogstraten-Miller, S.L., Kachar, B., Wu, D.K., Green, E.D., 2001. Targeted disruption of mouse Pds provides insight about the inner-ear defects encountered in Pendred syndrome. Hum. Mol. Genet. 10, 153–161.

Everett, L.A., Green, E.D., 1999. A family of mammalian anion transporters and their involvement in human genetic diseases. Hum. Mol. Genet. 8, 1883–1891.

Felsenstein, J., 1989. PHYLIP—Phylogeny Inference Package (Version 3.2). Cladistics 5, 164–166.

Forlino, A., Piazza, R., Tiveron, C., Della Torre, S., Tatangelo, L., Bonafe, L., Gualeni, B., Romano, A., Pecora, F., Superti-Furga, A., Cetta, G., Rossi, A., 2005. A diastrophic dysplasia sulfate transporter (SLC26A2) mutant mouse: morphological and biochemical characterization of the resulting chondrodysplasia phenotype. Hum. Mol. Genet. 14, 859–871.

Gu, X., 2001. A site-specific measure for rate difference after gene duplication or speciation. Mol. Biol. Evol. 18, 2327–2330.

Gu, X., Vander Velden, K., 2002. DIVERGE: phylogeny-based analysis for functional–structural divergence of a protein family. Bioinformatics 18, 500–501.

Guinan, J.J., 1996. In: Dallos, Popper, Fay, (Eds.), The Cochlea. Springer, New York, pp. 435–502.

Hoglund, P., Haila, S., Socha, J., Tomaszewski, L., Saarialho-Kere, U., Karjalainen-Lindsberg, M.L., Airola, K., Holmberg, C., de la Chapelle, A., Kere, J., 1996. Mutations of the down-regulated in adenoma (DRA) gene cause congenital chloride diarrhoea. Nat. Genet. 14, 316–319.

Hughes, A.L., Nei, M., 1988. Pattern of nucleotide substitution at major histocompatibility complex class I loci reveals overdominant selection. Nature 335, 167–170.

Jia, S., He, D.Z., 2005. Motility-associated hair-bundle motion in mammalian outer hair cells. Nat. Neurosci. 8, 1028–1034.

Jones, A.K., Elgar, G., Sattelle, D.B., 2003. The nicotinic acetylcholine receptor gene family of the pufferfish, *Fugu rubripes*. Genomics 82, 441–451.

Jones, D.T., Taylor, W.R., Thornton, J.M., 1992. The rapid generation of mutation data matrices from protein sequences. Comput. Appl. Biosci. 8, 275–282.

Karlin, A., 2002. Emerging structure of the nicotinic acetylcholine receptors. Nat. Rev. Neurosci. 3, 102–114.

Katz, E., Verbitsky, M., Rothlin, C.V., Vetter, D.E., Heinemann, S.F., Elgoyhen, A.B., 2000. High calcium permeability and calcium block of the alpha9 nicotinic acetylcholine receptor. Hear Res. 141, 117–128.

Kennedy, H.J., Crawford, A.C., Fettiplace, R., 2005. Force generation by mammalian hair bundles supports a role in cochlear amplification. Nature 433, 880–883.

Knudsen, B., Miyamoto, M.M., 2001. A likelihood ratio test for evolutionary rate shifts and functional divergence among proteins. Proc. Natl. Acad. Sci. USA 98, 14512–14517.

Kumar, S., Hedges, S.B., 1998. A molecular timescale for vertebrate evolution. Nature 392, 917–920.

Le Novere, N., Changeux, J.P., 1999. The Ligand Gated Ion Channel Database. Nucleic Acids Res. 27, 340–342.

Le Novere, N., Corringer, P.J., Changeux, J.P., 2002. The diversity of subunit composition in nAChRs: evolutionary origins, physiologic and pharmacologic consequences. J. Neurobiol. 53, 447–456.

Li, W.H., 1993. Unbiased estimation of the rates of synonymous and nonsynonymous substitution. J. Mol. Evol. 36, 96–99.

Liberles, D.A., 2001. Evaluation of methods for determination of a reconstructed history of gene sequence evolution. Mol. Biol. Evol. 18, 2040–2047.

Liberman, M.C., Gao, J., He, D.Z., Wu, X., Jia, S., Zuo, J., 2002. Prestin is required for electromotility of the outer hair cell and for the cochlear amplifier. Nature 419, 300–304.

Liu, X.Z., Ouyang, X.M., Xia, X.J., Zheng, J., Pandya, A., Li, F., Du, L.L., Welch, K.O., Petit, C., Smith, R.J., Webb, B.T., Yan, D., Arnos, K.S., Corey, D., Dallos, P., Nance, W.E., Chen, Z.Y., 2003. Prestin, a cochlear motor protein, is defective in non-syndromic hearing loss. Hum. Mol. Genet. 12, 1155–1162.

Lohi, H., Kujala, M., Makela, S., Lehtonen, E., Kestila, M., Saarialho-Kere, U., Markovich, D., Kere, J., 2002. Functional characterization of three novel tissue-specific anion exchangers SLC26A7, -A8, and -A9. J. Biol. Chem. 277, 14246–14254.

Manley, G.A., 2000. Cochlear mechanisms from a phylogenetic viewpoint. Proc. Natl. Acad. Sci. USA 97, 11736–11743.

Manley, G.A., Popper, A.N., Fay, R.R., 2004. Evolution of the Vertebrate Auditory System. Springer, New York.

Mount, D.B., Romero, M.F., 2004. The SLC26 gene family of multifunctional anion exchangers. Pflugers Arch. 447, 710–721.

Nei, M., Gojobori, T., 1986. Simple methods for estimating the numbers of synonymous and nonsynonymous nucleotide substitutions. Mol. Biol. Evol. 3, 418–426.

Nielsen, R., Yang, Z., 1998. Likelihood models for detecting positively selected amino acid sites and applications to the HIV-1 envelope gene. Genetics 148, 929–936.

Scott, D.A., Wang, R., Kreman, T.M., Andrews, M., McDonald, J.M., Bishop, J.R., Smith, R.J., Karniski, L.P., Sheffield, V.C., 2000. Functional differences of the PDS gene product are associated with phenotypic variation in patients with Pendred syndrome and non-syndromic hearing loss (DFNB4). Hum. Mol. Genet. 9, 1709–1715.

Scott, D.A., Wang, R., Kreman, T.M., Sheffield, V.C., Karniski, L.P., 1999. The Pendred syndrome gene encodes a chloride-iodide transport protein. Nat. Genet. 21, 440–443.

Sgard, F., Charpantier, E., Bertrand, S., Walker, N., Caput, D., Graham, D., Bertrand, D., Besnard, F., 2002. A novel human nicotinic receptor subunit, alpha10, that confers functionality to the alpha9-subunit. Mol. Pharmacol. 61, 150–159.

Soleimani, M., Greeley, T., Petrovic, S., Wang, Z., Amlal, H., Kopp, P., Burnham, C.E., 2001. Pendrin: an apical Cl-/OH-/HCO3-exchanger in the kidney cortex. Am. J. Physiol. Renal. Physiol. 280, F356–F364.

Thompson, J.D., Higgins, D.G., Gibson, T.J., 1994. CLUSTAL W: improving the sensitivity of progressive multiple sequence alignment through sequence weighting, position-specific gap penalties and weight matrix choice. Nucleic Acids Res. 22, 4673–4680.

Vetter, D.E., Liberman, M.C., Mann, J., Barhanin, J., Boulter, J., Brown, M.C., Saffiote-Kolman, J., Heinemann, S.F., Elgoyhen, A.B., 1999. Role of alpha9 nicotinic ACh receptor subunits in the development and function of cochlear efferent innervation. Neuron 23, 93–103.

Vincourt, J.B., Jullien, D., Amalric, F., Girard, J.P., 2003. Molecular and functional characterization of SLC26A11, a sodium-independent sulfate transporter from high endothelial venules. FASEB J. 17, 890–892.

Wang, Y., Gu, X., 2001. Functional divergence in the caspase gene family and altered functional constraints: statistical analysis and prediction. Genetics 158, 1311–1320.

Weber, T., Gopfert, M.C., Winter, H., Zimmermann, U., Kohler, H., Meier, A., Hendrich, O., Rohbock, K., Robert, D., Knipper, M., 2003. Expression of prestin-homologous solute carrier (SLC26) in auditory organs of nonmammalian vertebrates and insects. Proc. Natl. Acad. Sci. USA 100, 7690–7695.

Weisstaub, N., Vetter, D.E., Elgoyhen, A.B., Katz, E., 2002. The alpha9alpha10 nicotinic acetylcholine receptor is permeable to and is modulated by divalent cations. Hear. Res. 167, 122–135.

Yang, Z., 1997. PAML: a program package for phylogenetic analysis by maximum likelihood. Comput. Appl. Biosci. 13, 555–556.

Yang, Z., 1998. Likelihood ratio tests for detecting positive selection and application to primate lysozyme evolution. Mol. Biol. Evol. 15, 568–573.

Yang, Z., Nielsen, R., 2002. Codon-substitution models for detecting molecular adaptation at individual sites along specific lineages. Mol. Biol. Evol. 19, 908–917.

Yang, Z., Nielsen, R., Goldman, N., Pedersen, A.M., 2000. Codon-substitution models for heterogeneous selection pressure at amino acid sites. Genetics 155, 431–449.

Yang, Z., Swanson, W.J., 2002. Codon-substitution models to detect adaptive evolution that account for heterogeneous selective pressures among site classes. Mol. Biol. Evol. 19, 49–57.

Zheng, J., Du, G.G., Matsuda, K., Orem, A., Aguinaga, S., Deak, L., Navarrete, E., Madison, L.D., Dallos, P., 2005. The C-terminus of prestin influences nonlinear capacitance and plasma membrane targeting. J. Cell Sci. 118, 2987–2996.

Zheng, J., Shen, W., He, D.Z., Long, K.B., Madison, L.D., Dallos, P., 2000. Prestin is the motor protein of cochlear outer hair cells. Nature 405, 149–155.